Yousef, Mokhtar Ibrahim; Roychoudhury, Shubhadeep; Jafaar, Karrar Sabah; Slama, Petr; Kesari, Kavindra Kumar; Kamel, Maher Abd El-Nabi

Aluminum Oxide and Zinc Oxide Induced Nanotoxicity in Rat Brain, Heart, and Lung

Published in:
Physiological research

DOI:
10.33549/physiolres.934831

Published: 01/10/2022

Document Version
Publisher's PDF, also known as Version of record

Aluminum Oxide and Zinc Oxide Induced Nanotoxicity in Rat Brain, Heart, and Lung

Mokhtar Ibrahim YOUSEF[1], Shubhadeep ROYCHOUDHURY[2], Karrar Sabah JAFAAR[1], Petr SLAMA[3], Kavindra Kumar KESARI[4], Maher Abd El-Nabi KAMEL[5]

[1]Department of Environmental Studies, Institute of Graduate Studies and Research, Alexandria University, Alexandria, Egypt, [2]Department of Life Science and Bioinformatics, Assam University, Silchar, India, [3]Laboratory of Animal Immunology and Biotechnology, Department of Animal Morphology, Physiology, and Genetics, Faculty of AgriSciences, Mendel University in Brno, Brno, Czech Republic, [4]Department of Applied Physics, School of Science, Aalto University, Espoo, Finland, [5]Department of Biochemistry, Medical Research Institute, Alexandria University, Alexandria, Egypt

Received November 1, 2021
Accepted August 23, 2022
Epub Ahead of Print September 19, 2022

Summary

Nanomaterials or nanoparticles are commonly used in the cosmetics, medicine, and food industries. Many researchers studied the possible side effects of several nanoparticles including aluminum oxide (Al_2O_3-nps) and zinc oxide nanoparticles (ZnO-nps). Although, there is limited information available on their direct or side effects, especially on the brain, heart, and lung functions. This study aimed to investigate the neurotoxicity, cardiotoxicity, and lung toxicity induced by Al_2O_3-nps and ZnO-nps or in combination *via* studying changes in gene expression, alteration in cytokine production, tumor suppressor protein p53, neurotransmitters, oxidative stress, and the histological and morphological changes. Obtained results showed that Al_2O_3-nps, ZnO-nps and their combination cause an increase in 8-hydroxy-2´-deoxyguanosine (8-OHdG), cytokines, p53, oxidative stress, creatine kinase, norepinephrine, acetylcholine (ACh), and lipid profile. Moreover, significant changes in the gene expression of mitochondrial transcription factor-A (mtTFA) and peroxisome proliferator activator receptor-gamma-coactivator-1α (PGC-1α) were also noted. On the other hand, a significant decrease in the levels of antioxidant enzymes, total antioxidant capacity (TAC), reduced glutathione (GSH), paraoxonase 1 (PON1), neurotransmitters (dopamine – DA, and serotonin – SER), and the activity of acetylcholine esterase (AChE) in the brain, heart, and lung were found. Additionally, these results were confirmed by histological examinations. The present study revealed that the toxic effects were more when these nanoparticle doses are used in combination. Thus, Al_2O_3-nps and ZnO-nps may behave as neurotoxic, cardiotoxic, and lung toxic, especially upon exposure to rats in combination.

Key words

Aluminum oxide • Zinc oxide • Nanoparticles • Oxidative stress • Gene expression • Cytokines • p53 • Neurotransmitters • Histology

Corresponding authors

M. I. Yousef, Department of Environmental Studies, Institute of Graduate Studies and Research, Alexandria University, Alexandria 21526, Egypt. E-mail: yousefmokhtar@yahoo.com and S. Roychoudhury, Department of Life Science and Bioinformatics, Assam University, Silchar 788011, India. E-mail: shubhadeep1@gmail.com

Introduction

Aluminum oxide nanoparticles (Al_2O_3-nps) are generally found in skin care products, such as cosmetics [1]. Although, direct or oral exposure to Al_2O_3-nps may cause genotoxic effects [2]. Exposure to Al_2O_3-nps may produce reactive oxygen species (ROS) within the cells and impair the level of antioxidant activities [3]. Sarkar *et al.* also reported that Al_2O_3-nps generate ROS, which

can further result in increased pro-inflammatory reactions and oxidative stress [4]. Moreover, Al_2O_3-nps cause bioaccumulation in some organisms and result into harmful effects in the environment [5]. Al_2O_3-nps have been reported toxic in behavior [6], where they may induce oxidative stress and lead to oxidative damage of organs and tissues. Although, it depends on the exposure doses, where higher exposure doses of Al_2O_3-nps may induce free radical formation, leading to impaired inflammatory and blood-brain barrier (BBB) functions [7].

Zinc oxide nanoparticles (ZnO-nps) are commonly used in food industries and due to this, humans come in contact quite easily [8]. Their use particularly in the food packaging industry and as a source of food also leads to ZnO-nps consumption and entry to the human body [9]. Major sources of such exposure maybe from breathing, ingestion, or absorption by the gastrointestinal tract [10]. ZnO-nps enter the brain through the BBB and cause inflammation and cellular toxicity due to the formation of free radicals [11]. Exposure to high concentrations of ZnO-nps to the human epithelial cells results in the overproduction of ROS, which may also induce oxidative stress and lead to apoptosis and/or necrosis [12].

The present study aimed to explore the effects of Al_2O_3-nps and ZnO-nps alone or in combination on rat brain, heart, and lung functions. Several qualitative and quantitative studies including inflammatory cytokines, redox status, and gene expression (mitochondrial transcription factor-A – mtTFA; and peroxisome proliferator activator receptor-gamma-coactivator-1α – PGC-1α) were measured to investigate the cytotoxic and genotoxic role of nanoparticles

Methods

Tested compounds and doses

Al_2O_3-nps nanopowder (50 nm particle size) and ZnO-nps nanopowder (100 nm particle size), were purchased from Sigma-Aldrich (St. Louis, MO, USA). The doses were chosen based on the previous reports by Park *et al*. and Saman *et al*., where 70 mg/kg BW (dissolved in distilled water) dose of Al_2O_3-nps and 100 mg/kg BW of ZnO-nps were supplemented to the animals [13,14].

Animals and experimental groups

Forty (n=40) male Wistar rats (adult) of 5-6 months of age weighing 150-165 g were used in this study. Rats were acquired from the College of Medicine, Alexandria University, Egypt. The local animal ethics committee approved the design of the experiments, and the procedure was followed as per recommendations of the National Institutes of Health (NIH). Rats were housed in stainless-steel wire cages and provided a standard chow diet (53 % starch, 20 % protein, 9 % fat, 5 % fiber, purchased from Elfager Company, Alexandria, Egypt) with a tap drinking water supply. Rats were kept in a normal atmospheric condition where room temperature (25±5 °C) and humidity (50-60 %) were maintained throughout the experiments. After acclimation for fourteen days, rats were divided into four equal groups (n=10 for each group) as follows: a control group and 3 treated groups; groups 2, 3, and 4 which were orally gavaged with Al_2O_3-nps (70 mg/kg BW, dissolved in distilled water), ZnO-nps (100 mg/kg BW, dissolved in distilled water) and Al_2O_3-nps plus ZnO-nps (combined), respectively. Rats were administered orally the doses every day for 75 days.

Blood samples and tissue preparations

After 75 days the experiment was completed, and all the animals were sacrificed by cervical dislocation under deep anesthesia (ketamine 100 mg/kg and xylazine 10 mg/kg; intraperitoneally). Blood samples were collected by cardiac puncture from anesthetized animals in test tubes coated with heparin (as an anti-clotting agent) and immediately transferred into the ice. Thereafter, for the separation of plasma, the blood samples were centrifuged at 860×g for 20 min and stored at -80 °C until the analysis of the tested parameters. Furthermore, the brain, heart, and lungs were removed and washed with chilled saline solution, and the adhering fat and connective tissues were separated. The tissues were divided into 4 different groups for – 1) DNA isolation and 8-hydroxy-2´-deoxyguanosine (8-OHdG), 2) RNA isolation for gene expression analysis, 3) immersed immediately in formalin for histopathological examinations, and 4) minced and homogenized (10 %, w/v), separately, in ice-cold sucrose buffer (0.25 M) in a Potter-Elvehjem type homogenizer. Further, homogenates were centrifuged at 10000× g for 20 min at 4 C, to pellet the cell debris, and the supernatant was collected and stored at -80 °C which were used to determine the rest of the parameters.

Body and organs weights

The initial and final weights of animals were

recorded first and then, body weight gain (g/75 days) was calculated.

Body weight gain (g/75 days) = Final weight - Initial weight

The internal organs were detached and washed with chilled saline solution. Thereafter, the adhering lipid and connective tissues were detached and dried with tissue papers, and weights were calculated.

Quantitative analysis of gene expression of mitochondrial transcription factor A (mtTFA) and peroxisome proliferator activator receptor gamma-coactivator 1α (PGC-1α) using qRT-PCR

GF-1 total RNA extraction kit (Vivantis, Malaysia) was used to isolate total RNA from animals' tissues. In further steps, ViPrimePLUS one step quantitative real time reverse transcriptase-polymerase chain reaction (qRT-PCR) Green Master Mix (Vivantis, Malaysia) were used for the relative quantitative determination of the gene expression of mtTFA [15] and PGC-1α [16] at mRNA level using specific primer sequences as follow: β-actin; F: 5'-AGCCATGTACGTAGCCATCC-3' and R: 5'-CTCTCAGCTGTGGTGGTGAA-3', PGC-1α; F: 5'-AAACTTGCTAGCGGTCCTCA-3' and R: 5'-TGGCTGGTGCCAGTAAGAG-3', and mTFA; F: 5'CCCTGGAAGCTTTCAGATACG-3' and R: 5'-AATTGCAGCCATGTGGAGG-3'.

Assay of 8-hydroxy-2´-deoxyguanosine (8-OHdG)

GeneJet genomic DNA purification kit (Thermo Scientific, USA) was used to extract genomic DNA of tissues. The isolated DNA was digested by incubation with DNase I, nuclease P1 and alkaline phosphatase (Bio-Basic, Canada). The detailed protocol can be found from following link- 8-hydroxy-2-deoxyguanosine-elisa-kit-protocol-book-v6-ab201734 (website).pdf (abcam.com). Furthermore, 8-OHdG ELISA kit (ab201734, Abcam, Cambridge, UK) was used to measure 8-OHdG content in the resultant DNA hydrolysates, following the manufacturer's protocol.

Assay of lipid peroxidation

Lipid peroxidation has been found to result in the end-product of malondialdehyde (MDA). Therefore, MDA was determined by the thiobarbituric acid-reactive substances (TBARS) assay [17]. In this assay, MDA was heated with thiobarbituric acid (TBA) at a low pH to produce a pink chromogen with a maximum absorbance at 532 nm.

Assay of nitric oxide end products (nitrite and nitrate; NOx)

The concentration of nitrite and nitrate (NOx) end products in the deproteinized samples was determined *via* the Griess reaction. This reaction was supplemented with the reduction of nitrate to nitrite by NADPH-dependent nitrate reductase. This assay was performed in two steps: the first required the diazotization of sulphanilic acid with nitrite ions followed by the second step of coupling this product with a diamine, resulting in a measurable pink metabolite. This was measured at 540 nm [18].

ELISA

Rat ELISA kit (MyBioSource, San Diego, USA) was used to measure the tumor necrosis factor-alpha (TNF-α), tumor suppressor gene p53 and interleukin-6 (IL-6) in brain, heart, and lung tissue homogenates according to the manufacturer's instructions. Dopamine (DA), serotonin (SER), norepinephrine and acetylcholine (ACh) levels in plasma and brain tissues were assayed by using a competitive ELISA kit (Cloud-Clone Corp. Houston, USA).

Assay of antioxidants parameters

A number of factors were measured such as, colorimetric kits (Biodiagnostic, Egypt) for measuring of total antioxidant capacity (TAC) and the activities of superoxide dismutase (SOD), glutathione peroxidase (GP_X), glutathione S-transferase (GST) and catalase (CAT) in the tissue homogenates. Reduced glutathione (GSH) content was measured after protein precipitation using a metaphosphoric acid reagent. The assay was based on the oxidation of GSH by 5,5′-dithiobis-(2-nitrobenzoic acid) (DTNB) to yield glutathione disulfide (GSSG) and 5-thio-2-nitrobenzoic acid (TNB). The rate of TNB formation was assayed at 412 nm and, was also found proportional to the GSH present in the sample [19]. The rate of formation of TNB was monitored by recording the change in absorbance. This was found to be 412 nm per minute (ΔA/min). The total glutathione content in the samples was determined from a GSH standard curve and the results were subsequently expressed as nmol/g tissue by dividing the concentration of glutathione in the sample by the weight (in grams) of tissue used to prepare the sample.

Determination of paraoxonase (PON1) and creatine kinase cardiac muscle (CKCM) activities in the heart

Standard method [20] was followed to measure the paraoxonase (PON1) enzyme activity in the heart, and the creatine kinase in cardiac muscle (CKCM) by using an ELISA kit (BioVision, USA).

Lipid profile

Stored plasma samples were analyzed for total lipids, cholesterol, triacylglycerol (TAG) and high-density lipoprotein cholesterol (HDL-c) by using commercial kits (Biosystems, Barcelona, Spain). Low-density lipoprotein-cholesterol (LDL-c) was determined by the calculation [LDL-c = cholesterol - (HDL+ vLDL)]. Very low-density lipoprotein-cholesterol (vLDL-c) was calculated by dividing the values of the TAG with factor 5.

Histological preparation of brain, heart, and lung

Brain, heart, and lung specimens were obtained from rats and fixed in 10 % formalin before being treated with a conventional grade of alcohol and xylol, embedded in paraffin, and sectioned at 4-6 μm thickness. The sections were stained with hematoxylin and eosin (H&E) stain to study the histological changes [21].

Statistical analysis

Obtained data were summarized as means ± SE. The general linear model (GLM) was used to see the statistical differences within the group and parameters were analyzed by the GLM [22 SAS, 1998]. Duncan's New Multiple Range was used to test the significance of the differences between means, where values of $p<0.05$ were considered statistically significant [23].

Results

Body and organ weights

The results indicate no significant changes in the initial body weight (IBW) among the study groups. However, final body weight (FBW) and body weight gains (BWG) of the male rats treated with Al_2O_3-nps (70 mg/kg BW), ZnO-nps (100 mg/kg BW) or Al_2O_3-nps + ZnO-nps were significantly reduced ($p<0.05$) in comparison to the control group. Although, the differences were not significant among the three nanoparticles-treated groups. At the organ level, there were no significant differences in the weights of the brain and lung among all groups. However, heart weight was significantly lower ($p<0.05$) in all the nanoparticles-treated rats especially those treated with ZnO-nps alone or in combination with Al_2O_3-nps (Table 1).

Table 1. The body and organ weights of male rats treated with aluminum oxide nanoparticles (Al_2O_3-nps), zinc oxide nanoparticles (ZnO-nps) and their combination.

Weight (g)	**Experimental groups**			
	Control	**Al_2O_3-nps**	**ZnO-nps**	**Al_2O_3-nps + ZnO-nps**
IBW	169±3.17[a]	167±2.38[a]	170±2.24[a]	168±2.91[a]
FBW	222±6.16[a]	207±3.67[b]	201±5.50[b]	195±4.53[b]
BWG	53.5±8.45[a]	40±6.49[a, b]	30.5±6.97[b]	27±6.61[b]
Heart weight	0.81±0.10[a]	0.68±0.02[a, b]	0.65±0.02[b]	0.63±0.02[b]
Brain weight	1.52±0.07[a]	1.43±0.05[a]	1.41±0.04[a]	1.44±0.04[a]
Lung weight	1.63±0.06[a]	1.64±0.10[a]	1.57±0.07[a]	1.59±0.09[a]

Mean values within a row not sharing common superscript letters (a, b, c, d) were significantly different, $p<0.05$. IBW – initial body weight, FBW – final body weight, BWG – body weight gain.

Oxidative DNA damage

The genomic DNA contents of 8-OHdG in the brain, heart, and lung tissues of rats exposed to Al_2O_3-nps, ZnO-nps and their combination showed marked elevation ($p<0.05$) compared to the control tissues (Fig. 1). The highest levels of 8-OHdG were observed in the tissues of rats exposed to the combination of nanoparticles where whereas the highest-level changes were detected in the brain of rats treated with both nanoparticles (Fig. 1).

Gene expression of mtTFA and PGC-1α

Results showed significant downregulation of the expression of genes in the tissues regulating mitochondrial biogenesis and mtTFA function along with PGC-1α in rats exposed to Al_2O_3-nps, ZnO-nps individually and in combination (Fig. 2A, B). Moreover,

treatment with ZnO-nps showed a higher decrease in mtTFA and PGC-1α compared with Al_2O_3-nps ($p<0.05$). It shows that the suppression of brain, heart, and lung mtTFA and PGC-1α expression was more pronounced in the rats exposed to the combination of Al_2O_3-nps and ZnO-nps than each one alone.

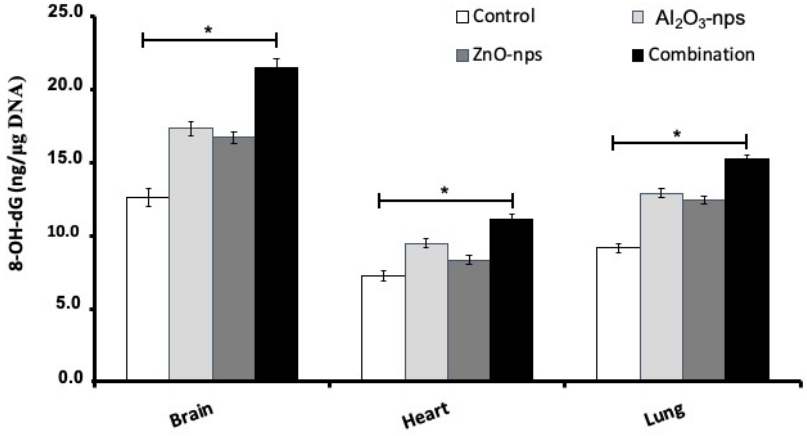

Fig. 1. The DNA content of 8-OHdG in the brain, heart and lung tissues of rats treated with aluminum oxide (Al_2O_3-nps) and zinc oxide nanoparticles (ZnO-nps) and their combination. 8-OH-dG: 8-hydroxydeoxyguanosine. Statistical analysis was performed to measure the significant differences with $p<0.05$ and has been denoted as [*]. The significant differences were compared to the control and the treatment groups.

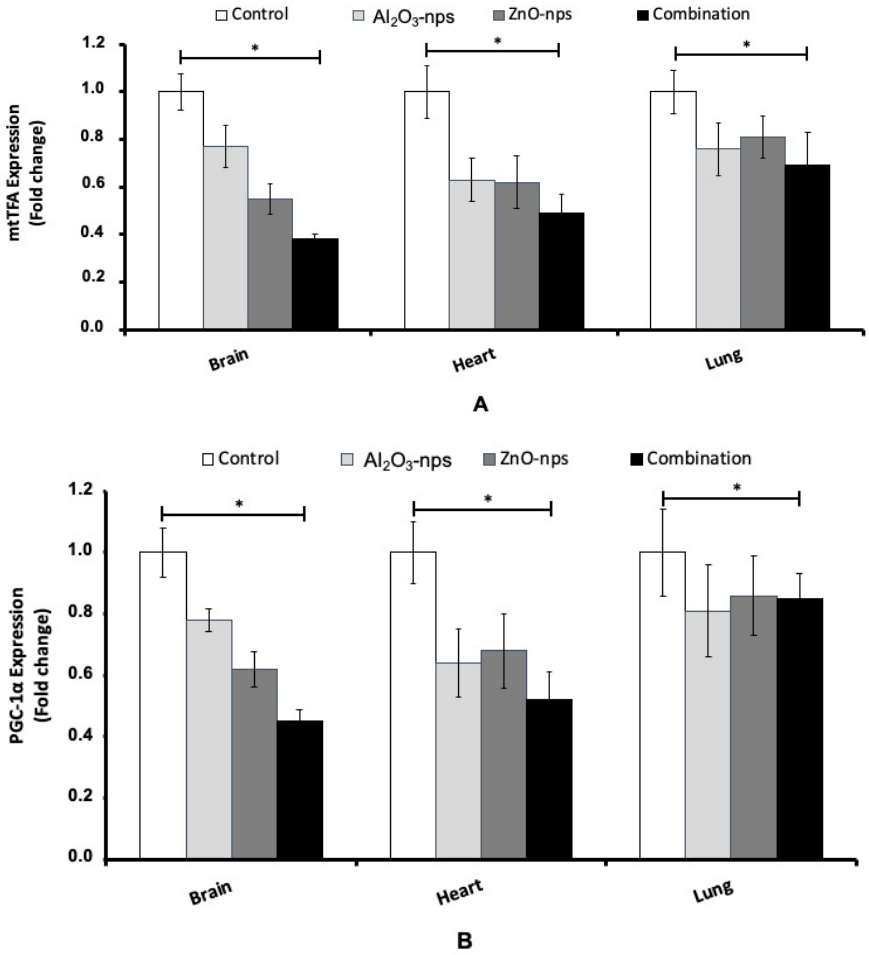

Fig. 2. The gene expression of mtTFA (**A**) and PGC-1α (**B**) in the brain, heart and lung tissues of rats treated with aluminum oxide nanoparticles (Al_2O_3-nps), zinc oxide nanoparticles (ZnO-nps), and their combination. Statistical analysis was performed to measure the significant differences with $p<0.05$ and has been denoted as [*]. The significant differences were compared in the control and the treatment groups.

Lipid peroxidation, oxidative stress, and antioxidants

Results showed significantly higher contents of TBARS, an index of lipid peroxidation, and NOx in the rats exposed to any of the used nanoparticles compared to control ($p<0.05$). The animals treated with the combination of Al_2O_3-nps and ZnO-nps showed significant elevation of TBARS and NOx compared to control rats and also treated by the individual nanoparticles (Table 2). On the other hand, all studied tissues showed a significant decline in the contents of GSH, TAC, and the activities of SOD, CAT, GPx and GST also decreased significantly ($p<0.05$) in the rats exposed to Al_2O_3-nps and/or ZnO-nps (with the lowest levels in the rats exposed to the combination of the nanoparticles used) (Table 2).

Table 2. The levels of glutathione (GSH), total antioxidant activity (TAC), nitric oxide (NO) and thiobarbituric acid-reactive substances (TBARS) and the activities of superoxide dismutase (SOD), catalase (CAT), glutathione peroxidase (GPx), and glutathione S-transferase (GST), in the brain, heart and lung tissues of male rats treated with aluminum oxide nanoparticles (Al_2O_3-nps), zinc oxide nanoparticles (ZnO-nps) and their combination.

Parameter	**Experimental group**			
	Control	**Al_2O_3-nps**	**ZnO-nps**	**Al_2O_3-nps + ZnO-nps**
Brain				
GSH (µmol/g tissue)	5.6±0.09^{a}	3.3±0.10^{b}	3.0±0.13^{b}	2.4±0.13^{c}
SOD (mU/mg protein)	49.3±2.6^{a}	28.4±2.8^{b}	13.2±0.8^{c}	8.0±0.8^{d}
CAT (mU/mg protein)	40±1.66^{a}	24±1.27^{b}	16±0.80^{c}	12±0.90^{d}
GPx (mU/mg protein)	56.5±3.20^{a}	41.3±2.1^{b}	32.3±1.15^{c}	20.9±2.38^{d}
GST (U/mg protein)	0.71±0.02^{a}	0.56±0.02^{b}	0.36±0.01^{c}	0.25±0.01^{d}
TAC (µM/g tissue)	20.03±0.36^{a}	17.40±0.25^{b}	14.51±0.39^{b}	12.37±0.54^{c}
NO (µmol/g tissue)	0.43±0.02^{d}	0.57±0.01^{c}	0.84±0.01^{b}	1.16±0.03^{a}
TBARS (nmol/g tissue)	35±0.9^{d}	62±0.6^{c}	73±3.3^{b}	90±0.8^{a}
Heart				
GSH (µmol/g tissue)	5.1±0.08^{a}	3.0±0.04^{b}	2.6±0.06^{c}	2.0±0.03^{d}
SOD (mU/mg protein)	28.7±2.6^{a}	25.7±2.8^{b}	13.3±1.2^{c}	8.6±0.8^{d}
CAT (mU/mg protein)	59±4.20^{a}	31±5.61^{b}	27±4.37^{b}	14±1.80^{c}
GPx (mU/mg protein)	56.3±1.738^{a}	34.6±0.647^{b}	24.8±1.255^{c}	17.2±0.417^{d}
GST (U/mg protein)	0.50±0.01^{a}	0.40±0.01^{b}	0.34±0.0^{c}	0.28±0.0^{c}
TAC (µM/g tissue)	2.31±0.15^{a}	1.73±0.05^{b}	1.71±0.03^{b}	1.38±0.01^{c}
NO (µmol/g tissue)	0.28±0.01^{c}	0.33±0.00^{c}	0.44±0.01^{b}	0.50±0.01^{a}
TBARS (nmol/g tissue)	61.9±0.9^{d}	104±0.7^{b}	90±2.1^{c}	113±0.5^{a}
Lung				
GSH (µmol/g tissue)	7.4±0.14^{a}	6.5±0.12^{b}	5.7±0.20^{c}	4.8±0.08^{d}
SOD (mU/mg protein)	10.4±0.6^{a}	6.0±0.8^{b}	4.7±0.8^{c}	3.8±0.2^{d}
CAT (mU/mg protein)	62±2.59^{a}	46±2.24^{b}	31±1.58^{c}	23±0.82^{d}
GPx (m/mg protein)	58.8±1.95^{a}	48.1±2.86^{b}	41.8±2.15^{c}	17.1±0.89^{d}
GST (U/mg protein)	0.75±0.0^{a}	0.51±0.01^{b}	0.49±0.0^{c}	0.40±0.0^{d}
TAC (µM/g tissue)	2.37±0.01^{a}	2.11±0.02^{b}	1.87±0.01^{c}	1.63±0.01^{d}
NO (µmol/g tissue)	0.4±0.01^{d}	0.5±0.01^{c}	0.7±0.01^{b}	0.8±0.01^{a}
TBARS (nmol/g tissue)	17±0.2^{d}	20±0.3^{c}	22±0.6^{b}	32±0.6^{a}

Mean values within a row not sharing common superscripts (a, b, c, d) were significantly different, $p<0.05$.

Inflammatory cytokines and p53

Results showed that treatment with Al_2O_3-nps and/or ZnO-nps caused a significant increase in the brain, heart, and lung p53, TNF and IL-6 levels in comparison with the control group ($p<0.05$). Although ZnO-nps were found more effective to induce these parameters compared with Al_2O_3-nps. The co-exposure of Al_2O_3-nps with ZnO-nps caused pronounced synergistic effects on p53, TNF-α and IL-6 compared to each one alone (Fig. 3A-C).

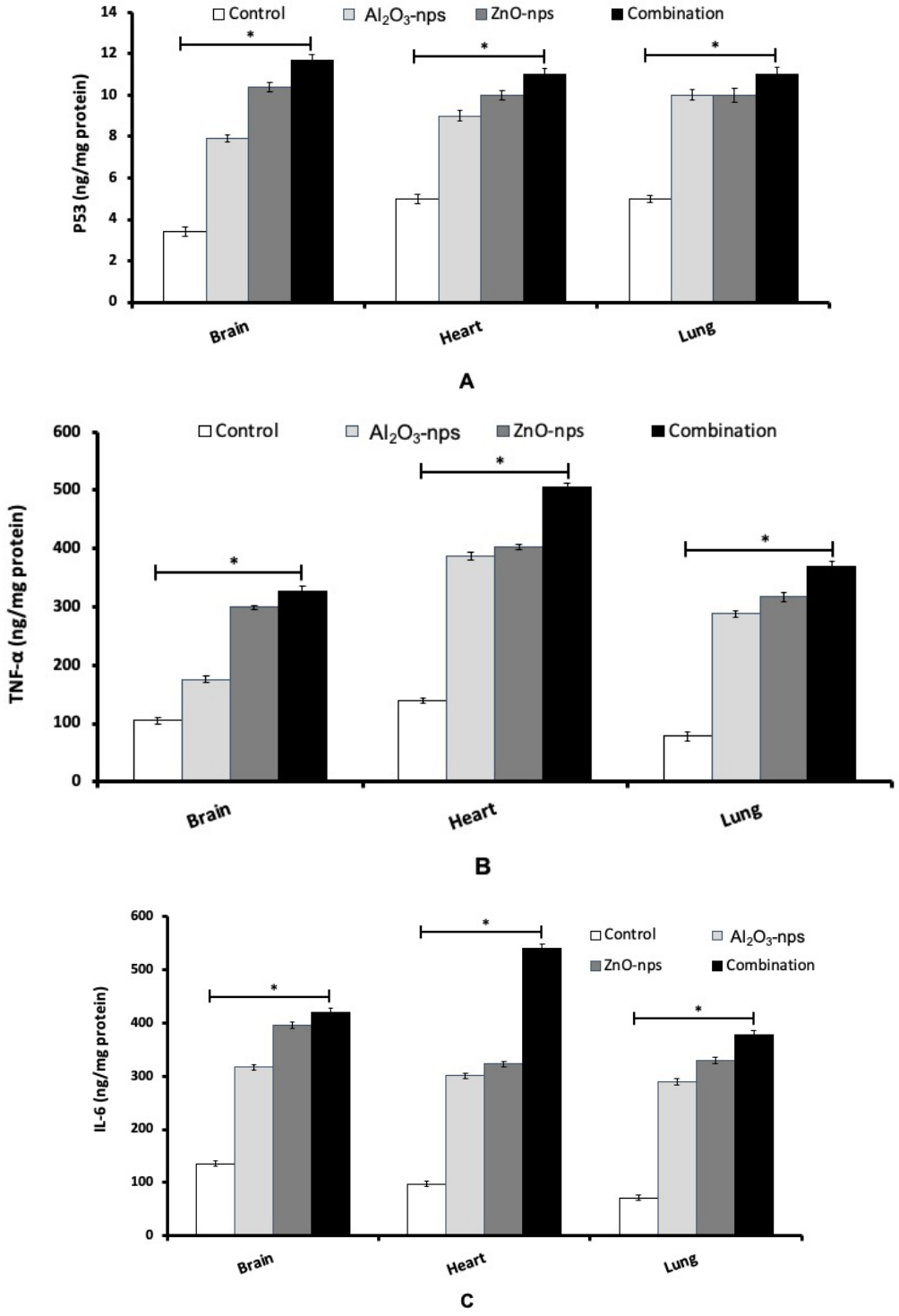

Fig. 3. The levels of p53 (**A**), and inflammatory cytokines TNF-α (**B**) and IL-6 (**C**) in the brain, heart, and lung tissues of rats treated with aluminum oxide nanoparticles (Al_2O_3-nps), zinc oxide nanoparticles (ZnO-nps), and their combination. TNF-α: Tumor necrosis factor-α; IL-6: interleukin-6. Statistical analysis was performed to measure the significant differences with $p<0.05$ and has been denoted as [*]. The significant differences were compared in the control and the treatment groups.

Brain and plasma neurotransmitters

The measurements showed that treatment with Al_2O_3-nps and ZnO-nps and their combination caused significant inhibition in plasma and brain activities of acetylcholinesterase (AChE), and significant elevation in the plasma and brain levels of ACh (Fig. 4A, B). Also, the levels of norepinephrine in the plasma and brain cortex were markedly raised in the nanoparticles exposed rats. On the other hand, the levels of DA and SER showed a significant increase in the plasma and brain compared to that of the control group (Fig. 5A-B). The level of norepinephrine also showed a significant difference ($p<0.05$) as compared to that of the control with an increase in brain but a decline in plasma (Fig. 5C). From the figures it may appear that ZnO-nps show a more prominent effect than Al_2O_3-nps regarding the levels of SER and norepinephrine while the reverse is true regarding the levels of ACh and DA. Furthermore, it may seem that the combination group showed a synergistic effect on the above parameters compared with each nanoparticle treatment (Figs 4 and 5).

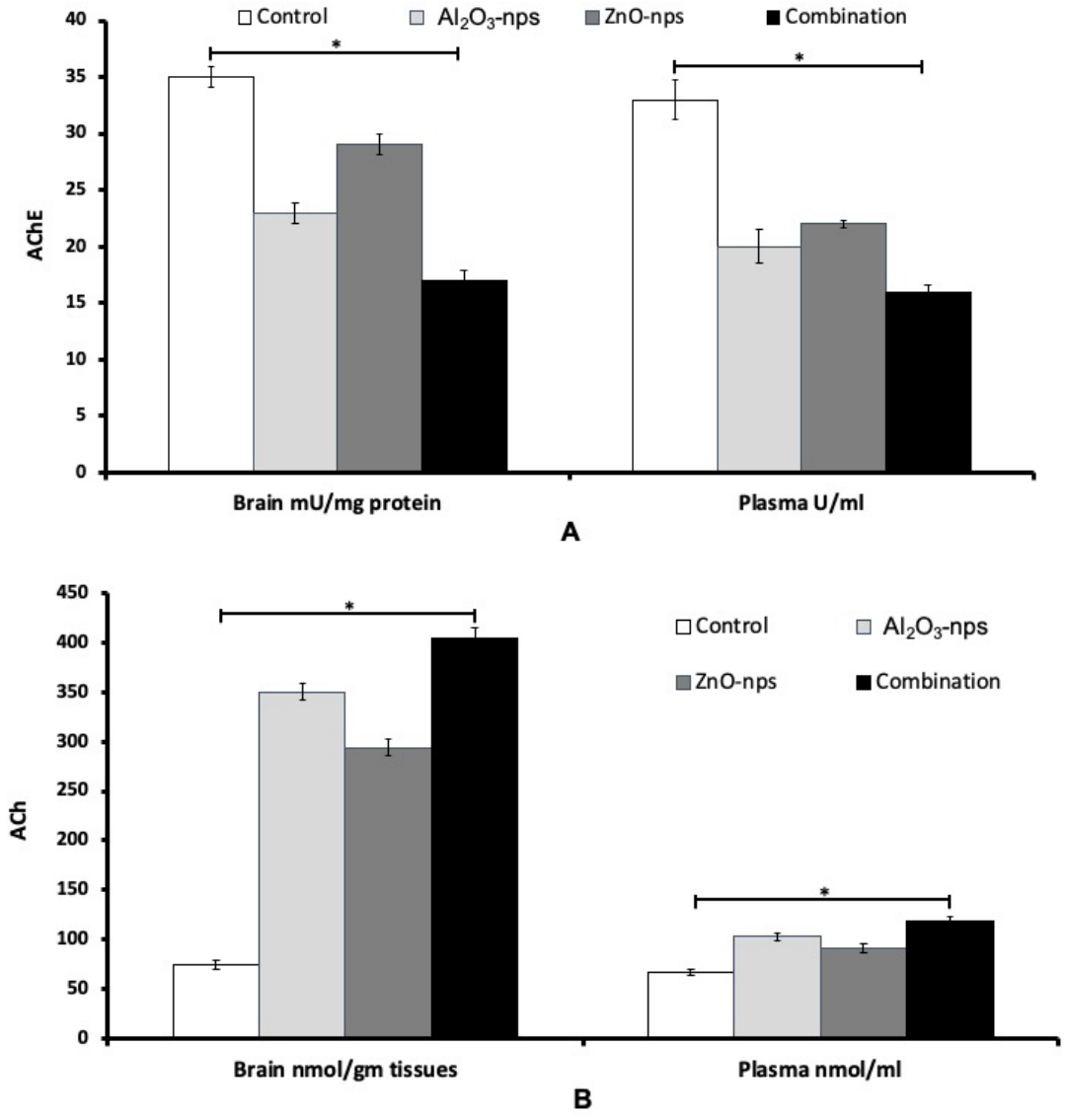

Fig. 4. The activity of acetylcholine esterase – AChE (**A**) and the level of acetylcholine – ACh (**B**) in the brain cortex and plasma of rats treated with aluminum oxide nanoparticles (Al_2O_3-nps), zinc oxide nanoparticles (ZnO-nps), and their combination. Statistical analysis was performed to measure the significant differences with $p<0.05$ and has been denoted as [*]. The significant differences were compared in the control and the treatment groups.

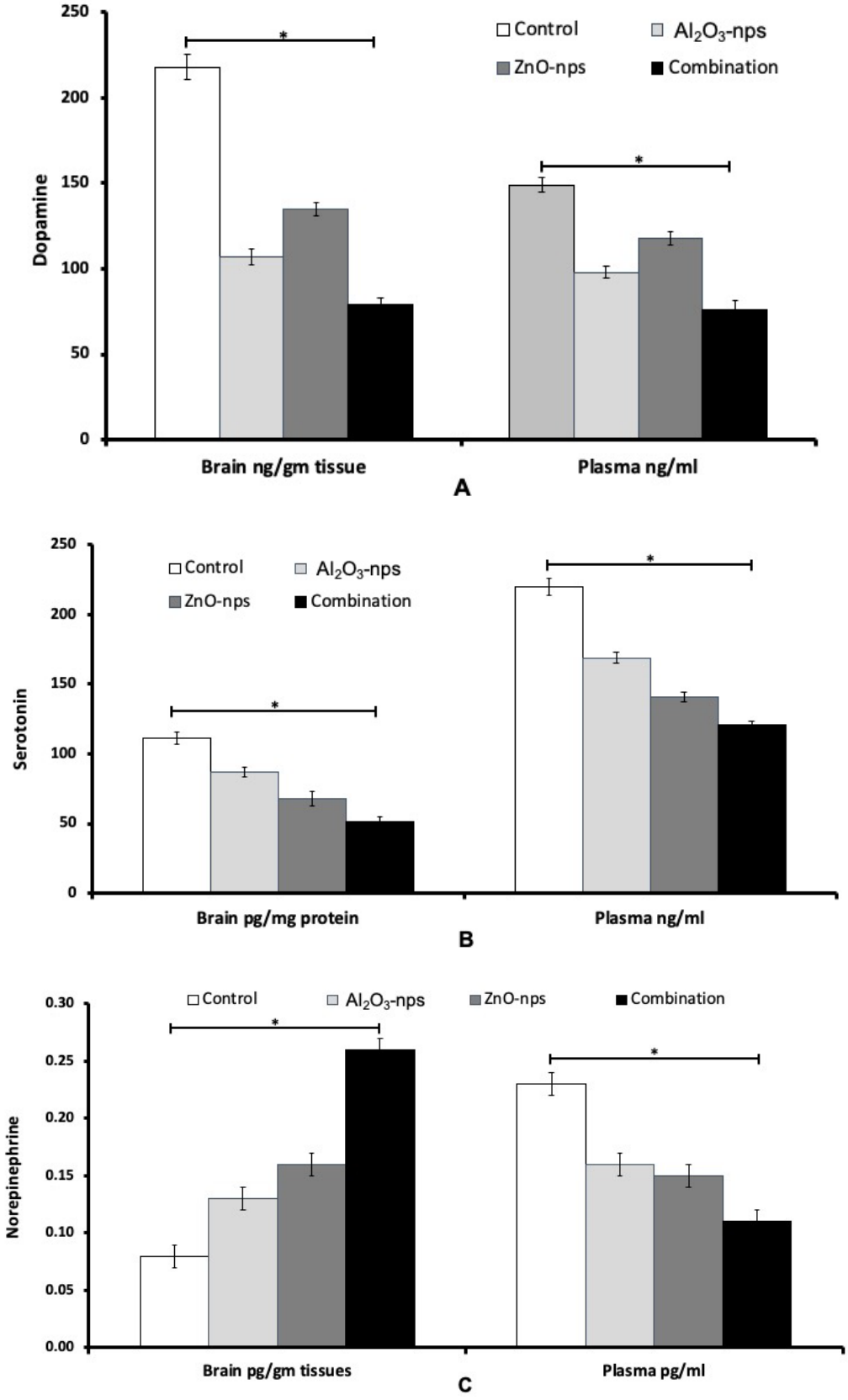

Fig. 5. Levels of dopamine (**A**), serotonin (**B**), and norepinephrine (**C**) in the brain cortex and plasma of rats treated with aluminum oxide nanoparticles (Al_2O_3-nps), zinc oxide nanoparticles (ZnO-nps), and their combination. Statistical analysis was performed to measure the significant differences with $p<0.05$ and has been denoted as [*]. The significant differences were compared to the control and between the treatment groups.

Cardiac muscle creatine kinase activity (CKCM) and paraoxonase (PON1) activity

The plasma and heart PON1 and CMCK enzyme activities of male rats treated with Al_2O_3-nps, ZnO-nps and their combination are presented in Figure 6A and 6B. Treatment with Al_2O_3-nps, ZnO-nps and their combination resulted in a significant decrease in PON1 and an increase in CMCK activities in plasma and heart compared to the control group ($p<0.05$). The individual treatment with ZnO-nps has found more prominent effects than Al_2O_3-nps. Although, combined treatment has been found to cause more pronounced effects compared to each treatment of nanoparticles (Fig. 6A, B).

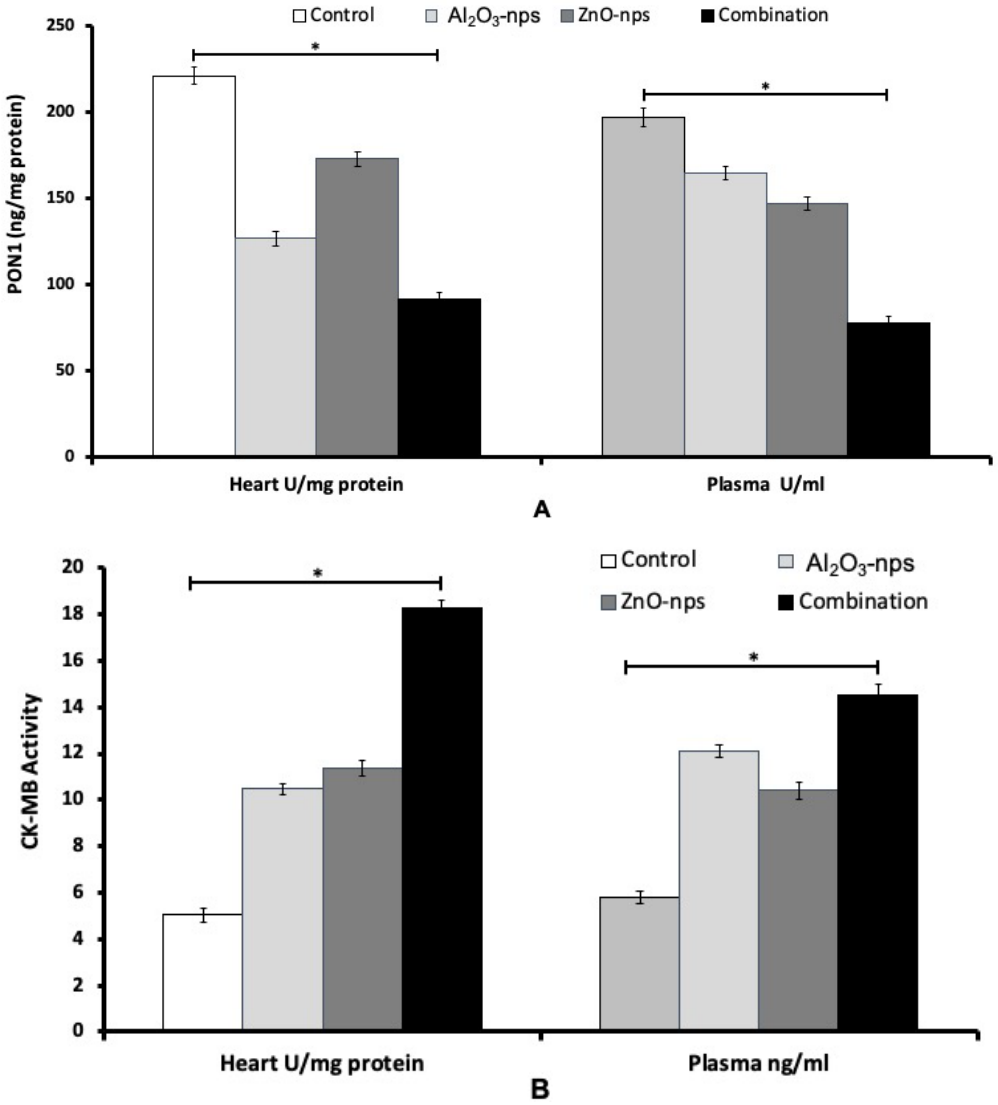

Fig. 6. The activities of paraoxonase 1 (PON1) (**A**) and CKCM (**B**) in the cardiac tissues and plasma of rats treated with zinc oxide nanoparticles (ZnO-nps), aluminum oxide nanoparticles (Al_2O_3-nps) and their combination. Statistical analysis was performed to measure the significant differences with $p<0.05$ and has been denoted as [*]. The significant differences were compared in the control and the treatment groups.

Lipid profile

Lipid profile data including the total lipids (TL), total cholesterol (TC), triglycerides (TG), HDL-c, LDL-c and vLDL-c are presented in Table 3. Measurements showed that the treatment with Al_2O_3-nps, ZnO-nps, and their combination produced a marked increase in the TL, TG, TC, LDL-c, and vLDL-c and a significant decrease in the level of HDL-c compared to the control group. The treatment with ZnO-nps appeared to show significant changes compared to Al_2O_3-nps. Also, it may seem that the treatment with the combination of nanoparticles showed significantly more pronounced effects than each nanoparticle treatment.

Table 3. Plasma lipid profiles of male rats treated with aluminum oxide nanoparticles (Al_2O_3-nps), zinc oxide nanoparticles (ZnO-nps), and their combination.

Parameter (mg/dl)	Experimental groups			
	Control	**Al_2O_3-nps**	**ZnO-nps**	**Al_2O_3-nps + ZnO-nps**
TL	533±4.6^{d}	843±30.9^{b}	738±28.9^{c}	986±53.2^{a}
TC	110±3.2^{c}	259±12.9^{b}	169±11.3^{c}	300±3.0^{a}
TG	144±1.13^{d}	174±5.41^{b}	164±1.65^{c}	197±1.48^{a}
HDL-c	46±0.92^{a}	33±0.67^{c}	38±0.75^{b}	26±0.35^{d}
LDL-c	35±3.31^{d}	166±2.02^{b}	78±3.77^{c}	234±5.53^{a}
vLDL-c	29±0.0^{d}	35±0.0^{b}	33±0.0^{c}	39±0.0^{a}

Mean values within a row not sharing a common superscript (a, b, c, d) were significantly different ($p<0.05$).

Brain histopathology

Microscopic examination of brain (cerebral cortex) sections of the control group (Fig. 7B1) demonstrated normal arrangements in layers – external granular, external pyramidal, inner granular, inner pyramidal, and polymorphic cell layers. These layers were lying towards the white matter (note, neuroglial cells) and seen within the homogenous compact acidophilic neurophil. While sections in the cerebral cortex of the ZnO-nps-exposed group showed disorganized cortical layers with widespread neuronal loss. The neurophil exhibited several fissures and small cysts. The pyramidal neurons shrunk with evident perineuronal edematous areas. They also showed neuronal degeneration, pyknosis of the nuclei with pericellular edema, dilation of blood vessels and vacuolization as seen in Figure 7 (B2) compared to the control group. Sections in the cerebral cortex of Al_2O_3-nps-treated group showed ill-defined cortical layers, too. The brain surface showed irregularity with a broad molecular layer and thick meninges. The pyramidal neurons are dark acidophilic pyknotic nuclei (note, multiple cysts of variable sizes were seen within the neurophil) seen in Figure 7 (B3) as compared to the control group. The histopathological observations in Al_2O_3-nps and ZnO-nps treated groups showed disorganized cortical layers with evident neuronal loss. The brain surface exhibited irregular depressed areas and thick meninges with cellular infiltrations. The neurophil showed spongiform vacuolations with severely shrunk neurons exhibiting dark cytoplasm as seen in Figure 7 (B4), compared to Al_2O_3-nps and ZnO-nps alone.

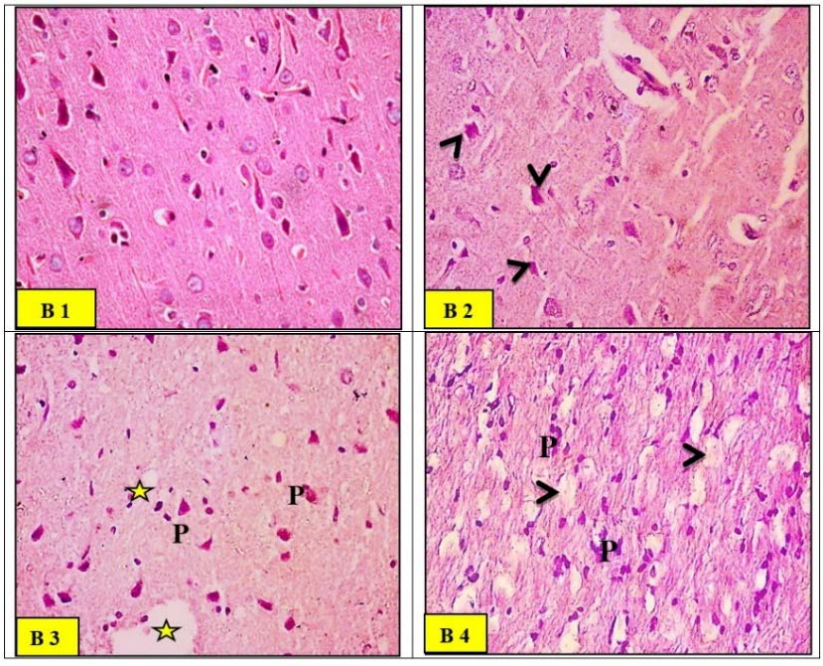

Fig. 7. Light micrographs of the control group (**B1**) rat brain (cerebral cortex) demonstrating normally arranged layers, external granular, external pyramidal, inner granular, inner pyramidal and polymorphic cell layer lying towards the white matter (note, neuroglial cells) were seen within the homogenous compact acidophilic neurophil. Light micrographs of zinc oxide nanoparticles (ZnO-nps) (**B2**) in rat brain showed disorganized cortical layers with widespread neuronal loss. The pyramidal neurons shrun (arrow heads) with evident perineuronal edematous areas. Light micrographs of aluminum oxide nano-particles (Al_2O_3-nps) group (**B3**) rat cerebral cortex showed ill-defined cortical layers. The pyramidal neurons (p) were dark acidophilic with pyknotic nuclei. Multiple cysts (*) of variable sizes were seen within the neurophil. Light micrographs of combination (ZnO-nps + Al_2O_3-nps) group (**B4**) rat brain showed disorganized cortical layers with evident neuronal loss. Neurophils showed spongiform vacuolations (arrowheads) with severely shrunken neurons (p) exhibiting dark cytoplasm (H&E stain. Microscopic magnification ×400).

Heart histopathology

The qualitative observations showed a normal histological pattern in the cardiac muscle fibers which exhibit acidophilic sarcoplasm and ran in different directions with branching and anastomosing (Fig. 8H1). The histological observations in the ZnO-nps-treated group showed a thin distorted cardiac muscle fiber with areas of fragmentation and complete fiber loss. Waviness and hyper-eosinophilia of myofibers were also noticed as shown in Figure 8 (H2). The histological observations in the Al_2O_3-nps-treated group showed variable alterations of the myocardium in the form of thin, distorted fibers with some areas of fragmentation, the interstitial spaces appeared wide with some foci of extravasation. Some fibers exhibited pale sarcoplasm, other fibers showed localized hyper-eosinophilia with pyknotic nuclei, as seen in Figure 8 (H3). ZnO-nps and Al_2O_3-nps treated groups showed widespread fragmentation and degeneration of cardiac muscle fibers. Large areas appeared with pale vacuolar content, and other areas of localized hyper-eosinophilic sarcoplasm with pyknotic nuclei were also seen in Figure 8 (H4).

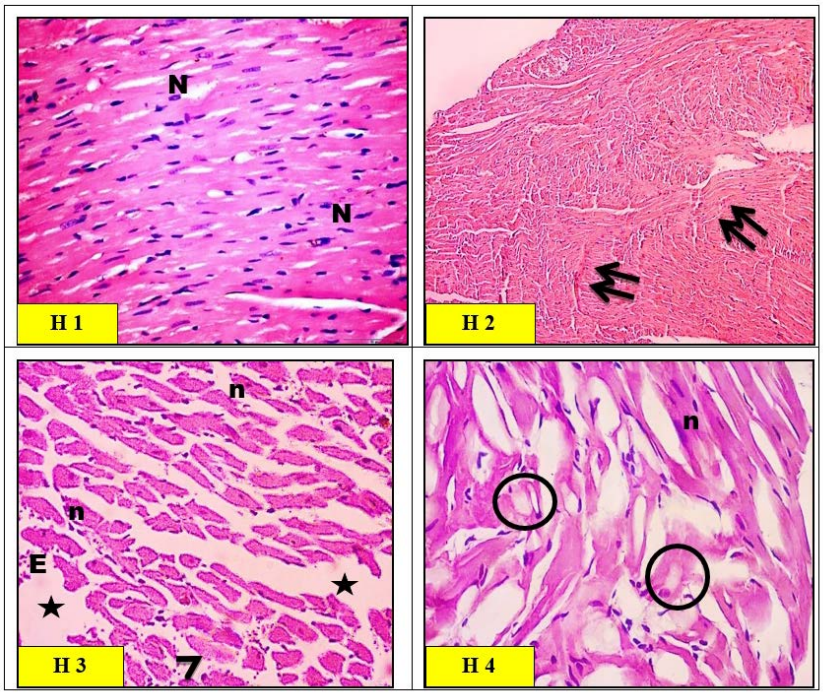

Fig. 8. Light micrographs of left ventricular myocytes of heart in control group (**H1**) rats showing a normal histological pattern. The cardiac muscle fibers exhibited acidophilic sarcoplasm and ran in different directions with branching and anastomosing. The cardiac muscle nuclei were vesicular and centrally located (N). Light micrographs of zinc oxide nanoparticles (ZnO-nps) group (**H2**) rat heart showed thin distorted cardiac muscle fibers with areas of fragmentation and complete fiber loss (arrows). Waviness and hypere-eosinophilia of myofibers were also noticed (double arrows). Light micrographs of aluminum oxide nanoparticles (Al_2O_3-nps) group (**H3**) rat heart showed the interstitial spaces appearing wide (*) with some foci of extravasation (E). Some fibers exhibited pale sarcoplasm (arrowhead), and other fibers showed localized hyper-eosinophilia with pyknotic nuclei (n). Light micrographs of combination (ZnO-nps + Al_2O_3-nps) group (**H4**) rat heart showed widespread fragmentation and degene-ration of cardiac muscle fibers. Large areas appear with pale vacuolar content (circles), and other areas of localized hypereosinophilic sarcoplasm with pyknotic nuclei (n) were also seen (H&E stain. Microscopic magnification ×400).

Lung histopathology

Micrographs of the control group rat lung showed a normal histological appearance of the alveolar tissue with patent alveoli and thin inter-alveolar septa (Fig. 9). High power view of the control rat alveolar tissue revealed pneumocytes. Moreover, a bronchiole with folded epithelium and part of the respiratory bronchiole, and a blood vessel was seen in Figure 9 (L1). Micrographs of the ZnO-nps treated group in rat lungs showed wide areas of collapsed and narrow alveoli. The interalveolar septa appeared thickened with an area of destruction and extruded cells into the alveolar lumina. Although, few foci have been found to exhibit emphysematous changes and destructed septa. Additionally, a wide patch of cellular infiltration has been noticed along with congested blood vessels as seen in Figure 9 (L2). Micrographs of Al_2O_3-nps treated group in rat lung showed areas of collapsed alveoli and thick interalveolar septa. Several areas demonstrated emphysematous changes with collapsed alveoli and ruptured walls. Pyknotic nuclei of degenerated cells in the interalveolar septa have been observed in Figure 9 (L3). Micrographs of combined treatment (ZnO-nps + Al_2O_3-nps) to rat lungs revealed that most of the alveolar tissues showed severe cellular infiltration and congested blood vessels as compared to the control group. Some alveoli revealed emphysematous changes, however, others collapsed. Area of hyalinization and vacuolation were depicted within the thickened interalveolar septa (Fig. 9L4).

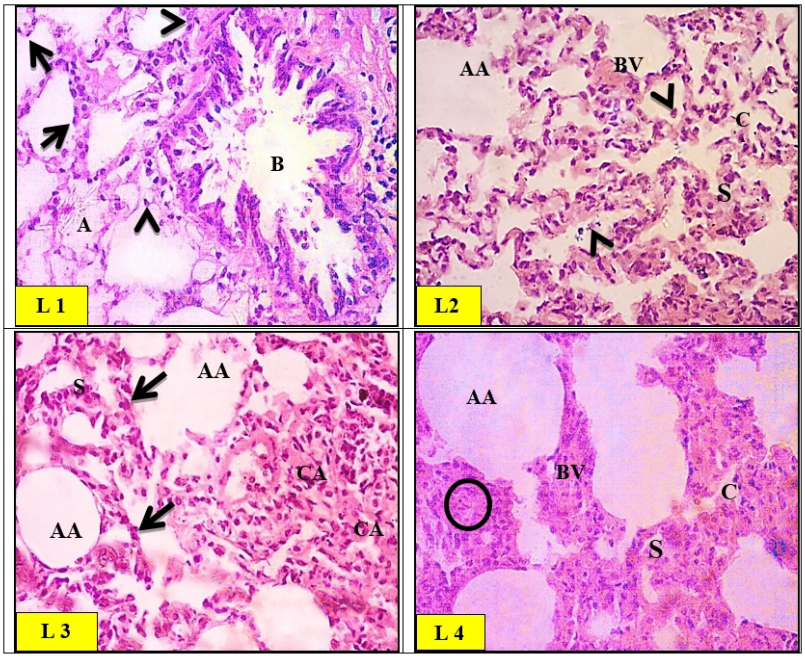

Fig. 9. Light micrographs of control (**L1**) group of rat lung showing a normal histological appearance of the alveolar tissue with patent alveoli (A) and thin inter-alveolar septa. High power view of the control rat alveolar tissue revealed pneumocytes type I (arrows) and type II (arrowheads). A bronchiole (B) with folded epithelium was also noticed. Light micrographs of zinc oxide nanoparticles (ZnO-nps) (**L2**) group of rat lung showed the interalveolar septa appearing thickened with an area of destruction and extruded cells into the alveolar lumina (arrowheads). Few foci exhibited emphysematous changes and destructed septa (AA). Congested blood vessels (BV) were also seen. Light micrographs of aluminum oxide nano-particles (Al_2O_3-nps) (**L3**) group of rat lung showed alternation with areas of collapsed alveoli (CA) and thick interalveolar septa (S). Several areas demonstrated emphysematous changes with collapsed alveoli and ruptured walls (AA). Pyknotic nuclei of degenerated cells in the interalveolar septa were noticed (Arrows). Light micrographs of the combi-nation (ZnO-nps + Al_2O_3-nps) (**L4**) group of rat lungs showed severe cellular infiltration (circles) and congested blood vessels (BV) as compared to the control group. Some alveoli revealed emphysematous changes (AA), and others were collapsed (CA). Areas of hyalinization and vacuolation are depicted within the thickened interalveolar septa (S) (H&E stain. Microscopic magnification ×400).

Discussion

The current study aimed to explore the nanotoxicity profile and general toxicity mechanism of Al_2O_3-nps or ZnO-nps alone, and their combination in rat brain, heart, and lung. Oral route for the administration of nanoparticles was opted for because it is the main route of exposure of these nanoparticles as they are being used in food packaging. Our study is also important because there are no guidelines available for conducting *in vivo* toxicity assessments. Therefore, the doses at which humans could be exposed to nanoparticles are unknown to date. The doses of nanoparticle treatment for this study have been selected based on available literature for studying sub-chronic oral toxicity. Although, baseline data has been utilized for the assessment of health hazards due to exposure to these metal oxide nanoparticles. The present study concludes that the oral administration with Al_2O_3-nps, ZnO-nps or their combi-nation for 75 consecutive days induced changes in the expression of genes regulating mitochondrial biogenesis, DNA oxidation, disturbed cytokine production, tumor suppressor protein p53, neurotransmitters and lipid peroxidation in rat brain, heart, and lung.

Previously, Al_2O_3-nps have been reported to affect genes due to their toxic nature [24]. However, exposure to ZnO-nps may lead to genotoxicity, and cellular toxicity, and proinflammatory cytokines are believed to play a role in it [25]. Recently, Yousef *et al.* reported that Al_2O_3-nps and ZnO-nps cause epigenetic and toxic alterations in the DNA and produce harmful effects in liver and kidney tissues [26].

Mitochondrial biogenesis plays a major role in conserving mitochondrial homeostasis to meet the physiological requirements of neuronal cells. The brain, heart, and lung are highly metabolic tissues with extreme demand for mitochondria in cardiac muscles and lung alveoli. The main regulators of mitochondrial biogenesis include mtTFA and PGC-1α – the essential controller of mitochondrial biogenesis [27]. Downregulated expression/function of PGC-1α and mtTFA were reported in neuron damage, which may lead to Parkinson's disease, Alzheimer's disease, and Huntington's disease [28]. Therefore, the downregulation effects of Al_2O_3-nps and ZnO-nps on brain PGC-1α implicate their exposure to susceptibility for the development of neurodegenerative diseases. In the current study, the lower expression of mtTFA and PGC-1α in the brain, heart, and lung tissues of rats exposed to Al_2O_3-nps and ZnO-nps might show a lowered mitochondrial biogenesis and replication of mtDNA and transcription that could cause dysfunction of mitochondria.

A number of molecules cannot transit through the BBB, which defends the brain from xenobiotics

penetration. However, the nanoparticles can overcome through BBB and get entry into the brain due to their particle size [29]. The suppressive influence of the used nanoparticles on the expression of mtTFA and PGC-1α can be suggestive of these nanoparticles' ability to enter through the BBB to reach the neuronal cells leading to induction of free radicals, oxidative stress, and lipid peroxidation as confirmed in our study.

Exposure to metallic nanoparticles such as Al_2O_3-nps and ZnO-nps are found at different industrial levels. These may come in contact quite easily with humans and start generating cellular oxidative stress. This was evident by elevated NOx, lipid peroxidation, and 8-OHdG and, also by a decline in GSH, TAC, and impaired antioxidant enzymes in the brain, heart, and lungs of rats. Several recent findings reported an increase in the intracellular ROS levels, induction of oxidative stress, and inflammation induced by Al_2O_3-nps toxicity [30-32]. Shah *et al.* also reported that Al_2O_3-nps are very toxic to human and mouse neuronal cells [33].

Yang *et al.* investigated that exposure to ZnO-nps may generate ROS and cellular oxidative stress [34]. Even small amounts of ZnO-nps integrated into cells may elevate the ROS formation [35]. Our results indicate elevated TBARS and NO levels in all the groups treated with nanoparticles clearly indicating oxidative stress in the brain, heart, and lungs of rats. Such oxidative stress may result from inducted ROS generation and/or impaired antioxidant systems. Although, organisms protect against the toxic impact of free radicals *via* the consumption of a different group of antioxidant enzymes. Our studies in the rat brain, heart, and lung have shown a significant inhibition in the antioxidant enzyme activities investigated (CAT, SOD, GST, and GPx) and reduced level of glutathione due to the exposure to Al_2O_3-nps and/or ZnO-nps.

Humans exposed to the nanoparticles may produce cellular toxicity and then DNA damage leading to hazard excess of cancer [36]. In the present study, the measurement of 8-OHdG has been found a good indicator of oxidative DNA damage. It showed a marked rise in brain, heart, and lung tissues as a product of the exposure to Al_2O_3-nps and/or ZnO-nps, and the level increased further when animals have been exposed to a combination of these nanoparticles. Alshatwi *et al.* reported that the Al_2O_3-nps may cause mitochondria-mediated cellular toxicity in human mesenchyme stem cells by producing free radicals [37]. Al_2O_3-nps induced neurotoxicity through impairments in learning behavior and mitochondrial dysfunctions, too [38].

The current study presented that Al_2O_3-nps and ZnO-nps alone or in combination may produce an increase in the tumor suppressor p53 and cytokines (IL-6 and TNF-α). In this connection, Riley *et al.* reported that the tumor suppressor p53 plays in part an essential role in the maintenance of cell cycle progression, differentiation, DNA repair, and apoptotic cell death [39]. This could be due to the excess production of ROS which may cause pro-inflammatory effect because it may activate the p53 and upregulate the IL-6 kinases and TNF-α [40]. Moreover, Turkez *et al.* reported that ROS can cause DNA destruction *via* activating p53 [41]. However, p53 plays an essential role in the maintenance of the genome through the inhibition of mutations [42].

Administration of Al_2O_3-nps and/or ZnO-nps disturbs the normal homeostasis of neurotransmitters as indicated by the inhibited activity of AChE and associated elevation of ACh in both plasma and brain cortex. Also, the exposure to studied nanoparticles caused a significant decline in DA and SER and a significant elevation in norepinephrine in both plasma and brain cortex. The most prominent effects were observed in the rats exposed to the combination of nanoparticles, which showed the synergism between them. The mechanism(s) of Al-induced neurotoxicity involves many interrelated pathways. *Rather et al.* reported that the size of Al^{3+} enables it to circulate through the body and cross the BBB and entry into brain cells thus accumulating in rat brain, especially in the hippocampus and cortex [43]. Functionally, Al can alter the BBB and produce alterations in the cholinergic and noradrenergic neurotransmission [44], which support to our present findings.

The neurotoxicity of Al_2O_3-nps also involves the serotonergic pathway as indicated by the significant decline of SER. SER is known to be found in several psychological conditions such as depression, anxiety, aggression, or psychosis. In line with this study, *post-mortem* AD brain demonstrated a decrease in SER, and its reduction in the cortex correlated with the neuronal loss at the raphe nuclei [45]. In line with our data, it was documented that metal oxide nanoparticles (TiO_2, ZnO, and Al_2O_3) cause an increase in the level of norepinephrine in the cortex region of the mouse brain thus leading to an inability to conserve an appropriate activity in the central nervous system because of their toxic nature [3]. Our results suggest that accumulation of

Al_2O_3-nps and ZnO-nps in the brain may cause changes in the production and release of certain neurotransmitters leading to neural damage, mitochondrial dysfunction, neuroinflammation, and oxidative stress that showed in histological changes in the brain architecture.

Regarding the cardiovascular system, our results showed that exposure to Al_2O_3-nps and/or ZnO-nps have atherogenic risk as indicated by the decline in the cardiac and plasma PON1 activity and elevated CKCM activity. Also, the exposures markedly affect the plasma lipid profile as indicated by elevated TL, TC, TG, and LDL-C and a decline in HDL-C (dyslipidemia). PON1 is a hydrolytic enzyme able to decrease the hazard of cardiovascular diseases through the reduction of the oxidation of LDL and lipid peroxidation [46].

The decline of PON1 and dyslipidemia in rats documented in this study might have led to atherogenic and cardiovascular diseases. This danger is shown in the current study by a marked rise of plasma and cardiac activities of CKCM and histological distortions of cardiac tissues such as myocardial congestion and damage. Moreover, the high plasma activity of CKCM is an indication of the injury to myocardium. Brook *et al.* also reported that the uptake to nanoparticles may cause health hazards and lead to cardiovascular diseases [47]. These nanoparticles possibly translocate through the air to the circulation and generate free radicals, trigger inflammation, vasomotor dysfunction, and neuronal signaling [48]. Also, in agreement with the obtained data, exposure to ZnO-nps *via* inhalation have been reported to lead to reactive acute alveolar inflammation in the lungs [49].

The present results of histological changes in the brain are in a similar range with the results of Shrivastava *et al.* [3], where the accumulation of metal oxide nanoparticles (ZnO and Al_2O_3) in the brain were found to cause neural damage through a change in the production and release of central neurotransmitters and receptors in the nerve. Moreover, the present results of heart histological changes are in agreement with those of Brook *et al.* who found that contact with nanoparticles are capable to cause health hazards such as cardiovascular diseases [47]. Also, the present observations of the histological changes are in the same line as that of Kreyling *et al.* who reported that the exposure to nanoparticles via inhalation may enter the lungs, where they may translocate to the circulatory system and lead to cardiovascular injuries [50].

Obtained results have therefore revealed the adverse impact of long-term exposure to Al_2O_3-nps and ZnO-nps in the brain, heart, and lung tissues. The neuro-, cardio- and lung toxicities were prompted through different pathways such as impaired mitochondrial biogenesis, oxidative DNA modification, inflammation, generation of free radicals, and reduction of antioxidant enzymes. Moreover, nanoparticles led to inauspicious changes in the tissue histology and lipid profile. So, the results indicate that concurrent co-exposure to Al_2O_3-nps and ZnO-nps lead to greater effects on the brain, heart, and lungs in comparison to the effect of each nanoparticles acting alone. The possible damaging effects of co-exposure to nanoparticles to other organs of the rat should be studied in the future, especially on the liver, kidney, and male reproductive organs.

Conclusions

Al_2O_3-nps and ZnO-nps alone and in combination induced neurotoxicity, cardiotoxicity, and pulmonary toxicity via increased 8-OHdG, decreased mtTFA and PGC-1α levels. These may also induce the inflammatory pathways through increased production of p53, TNF-α, and IL-6, generation of free radicals, oxidative stress, lipid peroxidation, imbalance in neurotransmitters, CKCM, PON1, lipid profile and destructive effects of histological changes. The neurotoxicity, cardiotoxicity, and pulmonary toxicity induced by the combination of Al_2O_3-nps and ZnO-nps appeared to be more pronounced than each one alone and these nanotoxicities result from the possible synergistic effect of metal oxide nanoparticles.

Conflict of Interest

There is no conflict of interest.

Abbreviations

ACh – acetylcholine, AChE – acetylcholinesterase, AD – after death, Al_2O_3-nps – aluminum oxide nanoparticles, BBB – blood-brain barrier, BW – body weight, BWG – body weight gain, CAT – catalase, CKCM – creatine kinase in cardiac muscle, DA – dopamine, DNA – deoxyribonucleic acid, DNase I – deoxyribonuclease I, DTNB – 5,5′-dithiobis-(2-nitrobenzoic acid), ELISA – enzyme-linked immunosorbent assay, FBW – final body weight, GLM – general linear model, GP_X – glutathione peroxidase, GSH – reduced glutathione, GSSG – glutathione disulphide, GST – glutathione S-transferase, HDL-c – high-density lipoprotein cholesterol, H&E –

haematoxylin and eosin, IBW – initial body weight, IL – interleukin, LDL-c – low-density lipoprotein-cholesterol, MDA – malondialdehyde, mRNA: messenger ribonucleic acid, mtDNA – mitochondrial DNA, mtTFA – mitochondrial transcription factor-A, NADPH – nicotinamide adenine dinucleotide phosphate, NO – nitric oxide, NOx – nitrite and nitrate, PGC-1α – peroxisome proliferator activator receptor gamma-coactivator-1α, PON1 – paraoxonase enzyme activity, p53 – a protein encoded by the gene *tumor protein P53 (TP53)*, qRT-PCR – quantitative real time reverse transcriptase-polymerase chain reaction, RNA – ribonucleic acid, ROS – reactive oxygen species, SAS – Statistical Analysis Systems Institute, SER – serotonin, SOD – superoxide dismutase, TAC – total antioxidant capacity, TAG – triacylglycerol, TBA – thiobarbituric acid, TBARS – thiobarbituric acid-reactive substances, TNB – 5-thio-2-nitrobenzoic acid, TNF-α – tumor necrosis factor-alpha, TC – total cholesterol, TL – total lipids, TG – triglycerides, vLDL-c – very low-density lipoprotein-cholesterol, ZnO-nps – zinc oxide nanoparticles, 8-OHdG – 8-hydroxy-2´-dexoyguanosine.

References

1. Poborilova Z, Opatrilova R, Babula P. Toxicity of aluminium oxide nanoparticles demonstrated using a BY-2 plant cell suspension culture model. Environ Exp Bot 2013;91:1-11. https://doi.org/10.1016/j.envexpbot.2013.03.002
2. Balasubramanyam A, Sailaja N, Mahboob M, Rahman MF, Misra S, Hussain SM, Grover P. Evaluation of genotoxic effects of oral exposure to aluminum oxide nanomaterials in rat bone marrow. Mutat Res Genet Toxicol Environ Mutagen 2009;676:41-47. https://doi.org/10.1016/j.mrgentox.2009.03.004
3. Shrivastava R, Raza S, Yadav A, Kushwaha P, Flora SJ. Effects of sub-acute exposure to TiO2, ZnO and Al2O3 nanoparticles on oxidative stress and histological changes in mouse liver and brain. Drug Chem Toxicol 2014;37:336-347. https://doi.org/10.3109/01480545.2013.866134
4. Sarkar A, Ghosh M, Sil PC. Nanotoxicity: oxidative stress mediated toxicity of metal and metal oxide nanoparticles. J Nanosci Nanotechnol 2014;14:730-743. https://doi.org/10.1166/jnn.2014.8752
5. Stanley JK, Coleman JG, Weiss CA Jr, Steevens JA. Sediment toxicity and bioaccumulation of nano and micron-sized aluminum oxide. Environ Toxicol Chem 2010;29:422-429. https://doi.org/10.1002/etc.52
6. Morsy GM, Abou El-Ala KS, Ali AA. Studies on fate and toxicity of nanoalumina in male albino rats: oxidative stress in the brain, liver and kidney. Toxicol Ind Health 2016;32:200-214. https://doi.org/10.1177/0748233713498462
7. Lockman PR, Koziara JM, Mumper RJ, Allen DD. Nanoparticle surface charges alter blood-brain barrier integrity and permeability. J Drug Target 2004;12:635-641. https://doi.org/10.1080/10611860400015936
8. Umrani RD, Paknikar KM. Zinc oxide nanoparticles show antidiabetic activity in streptozotocin-induced type 1 and 2 diabetic rats. Nanomedicine (Lond) 2014;9:89-104. https://doi.org/10.2217/nnm.12.205
9. Ansar S, Abudawood M, Hamed SS, Aleem MM. Exposure to zinc oxide nanoparticles induces neurotoxicity and proinflammatory response: amelioration by hesperidin. Biol Trace Elem Res 2017;175:360-366. https://doi.org/10.1007/s12011-016-0770-8
10. Vandebriel RJ, De Jong WH. A review of mammalian toxicity of ZnO nanoparticles. Nanotechnol Sci Appl 2012;5:61-71. https://doi.org/10.2147/NSA.S23932
11. Yang X, Jiang MZ. Research progress on biological toxicity of zinc oxide nanoparticle and its mechanism. (Article in Chinese) Zhejiang Da Xue Xue Bao Yi Xue Ban 2014;43:218-226. https://doi.org/10.3785/j.issn.1008-9292.2014.03.016
12. Premanathan M, Karthikeyan K, Jeyasubramanian K, Manivannan G. Selective toxicity of ZnO nanoparticles toward Gram-positive bacteria and cancer cells by apoptosis through lipid peroxidation. Nanomedicine 2011;7:184-192. https://doi.org/10.1016/j.nano.2010.10.001
13. Park EJ, Kim H, Kim Y, Choi K. Repeated-dose toxicity attributed to aluminum nanoparticles following 28-day oral administration, particularly on gene expression in mouse brain. Toxicol Environ Chem 2011;93:120-133. https://doi.org/10.1080/02772248.2010.495191

14. Saman S, Moradhaseli S, Shokouhian A, Ghorbani M. Histopathological effects of ZnO nanoparticles on liver and heart tissues in Wistar rats. Adv Biores 2013;4:83-88.
15. Piantadosi CA, Suliman HB. Mitochondrial transcription factor A induction by redox activation of nuclear respiratory factor 1. J Biol Chem 2006;281:324-333. https://doi.org/10.1074/jbc.M508805200
16. Li L, Pan R, Li R, Niemann B, Aurich AC, Chen Y, Rohrbach S. Mitochondrial biogenesis and peroxisome proliferator-activated receptor-γ coactivator-1α (PGC-1α) deacetylation by physical activity: intact adipocytokine signaling is required. Diabetes 2011;60:157-167. https://doi.org/10.2337/db10-0331
17. Draper HH, Hadley M. Malondialdehyde determination as index of lipid Peroxidation. Methods Enzymol 1990;186:421-431. https://doi.org/10.1016/0076-6879(90)86135-I
18. Guevara I, Iwanejko J, Dembinska-Kiec A, Pankiewicz J, Wanat A, Anna P, Golabek I, Bartus S, Malczewska-Malec M, Szczudlik A. Determination of nitrite/nitrate in human biological material by the simple Griess reaction. Clinica Chimica Acta 1998;274:177-188. https://doi.org/10.1016/S0009-8981(98)00060-6
19. Griffith OW. Determination of glutathione and glutathione disulfide using glutathione reductase and 2-vinylpyridine. Anal Biochem 1980;106:207-212. https://doi.org/10.1016/0003-2697(80)90139-6
20. Mueller RF, Hornung S, Furlong CE, Anderson J, Giblett ER, Motulsky AG. Plasma paraoxonase polymorphism: a new enzyme assay, population, family, biochemical, and linkage studies. Am J Hum Genet 1983;35:393-408.
21. Drury RA, Wallington EA: *Carleton's Histological Techniques*. Oxford University Press, New York, 1980, 520 p.
22. Statistical Analysis System. SAS Procedure Guide. Release 6.03 Edition. SAS Institute Inc., Cary, NC, USA, 1998.
23. Duncan DB. Multiple range and multiple F tests. Biometrics 1955;11:1-42. https://doi.org/10.2307/3001478
24. Balasubramanyam A, Sailaja N, Mahboob M, Rahman MF, Hussain SM, Grover P. In vivo genotoxicity assessment of aluminium oxide nanomaterials in rat peripheral blood cells using the comet assay and micronucleus test. Mutagenesis 2009;24:245-251. https://doi.org/10.1093/mutage/gep003
25. Hackenberg S, Zimmermann F-Z, Scherzed A, Friehs G, Froelich K, Ginzkey C, Koehler C, Burghartz M, Hagen R, Kleinsasser N. Repetitive exposure to zinc oxide nanoparticles induces DNA damage in human nasal mucosa mini organ cultures. Environ Mol Mutagen 2011;52:582-589. https://doi.org/10.1002/em.20661
26. Yousef MI, Mutar TF, Kamel MAEN. Hepato-renal toxicity of oral sub-chronic exposure to aluminum oxide and/or zinc oxide nanoparticles in rats. Toxicol Rep 2019;6:336-346. https://doi.org/10.1016/j.toxrep.2019.04.003
27. Wu Z, Puigserver P, Andersson U, Zhang C, Adelmant G, Mootha V, Troy A, Cinti S, Lowell B, Scarpulla RC, Spiegelman BM. Mechanisms controlling mitochondrial biogenesis and respiration through the thermogenic coactivator PGC-1. Cell 1999;98:115-124. https://doi.org/10.1016/S0092-8674(00)80611-X
28. Chaturvedi RK, Beal MF. Mitochondrial diseases of the brain. Free Radic Biol Med 2013;63:1-29. https://doi.org/10.1016/j.freeradbiomed.2013.03.018
29. Koziara JM, Lockman PR, Allen DD, Mumper RJ. The blood-brain barrier and brain drug delivery. J Nanosci Nanotechnol 2006;6:2712-2735. https://doi.org/10.1166/jnn.2006.441
30. Dong E, Wang Y, Yang ST, Yuan Y, Nie H, Chang Y, Wang L, Liu Y, Wang, H. Toxicity of nano gamma alumina to neural stem cells. J Nanosci Nanotechnol 2011;11:7848-7856. https://doi.org/10.1166/jnn.2011.4748
31. Prabhakar PV, Reddy UA, Singh SP, Balasubramanyam A, Rahman MF, Indu Kumari S, Agawane SB, Murty USN, Grover P, Mahboob M. Oxidative stress induced by aluminum oxide nanomaterials after acute oral treatment in Wistar rats. J Appl Toxicol 2012;32:436-445. https://doi.org/10.1002/jat.1775
32. Chen L, Zhang B, Toborek M. Autophagy is involved in nanoalumina-induced cerebrovascular toxicity. Nanomedicine 2013;9:212-221. https://doi.org/10.1016/j.nano.2012.05.017
33. Shah SA, Yoon GH, Ahmad A, Ullah F, Amin FU, Kim MO. Nanoscale-alumina induces oxidative stress and accelerates amyloid beta (Aβ) production in ICR female mice. Nanoscale 2015;7:15225-15237. https://doi.org/10.1039/C5NR03598H
34. Yang H, Liu C, Yang D, Zhang H, Xi Z. Comparative study of cytotoxicity, oxidative stress and genotoxicity induced by four typical nanomaterials: the role of particle size, shape and composition. J Appl Toxicol 2009;29:69-78. https://doi.org/10.1002/jat.1385

35. Toduka Y, Toyooka T, Ibuki Y. Flow cytometric evaluation of nanoparticles using side-scattered light and reactive oxygen species-mediated fluorescence-correlation with genotoxicity. Environ Sci Technol 2012;46:7629-7636. https://doi.org/10.1021/es300433x
36. Love SA, Maurer-Jones MA, Thompson JW, Lin YS, Haynes CL. Assessing nanoparticle toxicity. Annual Rev Anal Chem (Palo Alto Calif) 2012;5:181-205. https://doi.org/10.1146/annurev-anchem-062011-143134
37. Alshatwi AA, Subbarayan PV, Ramesh E, Al-Hazzani AA, Alsaif MA, Alwarthan AA. Aluminium oxide nanoparticles induce mitochondrial-mediated oxidative stress and alter the expression of antioxidant enzymes in human mesenchymal stem cells. Food Addit Contam Part A Chem Anal Control Expo Risk Assess 2013;30:1-10. https://doi.org/10.1080/19440049.2012.729160
38. Zhang QL, Li MQ, Ji JW, Gao FP, Bai R, Chen CY, Wang ZW, Zhang C, Niu Q. In vivo toxicity of nano-alumina on mice neurobehavioral profiles and the potential mechanisms. Int J Immunopathol Pharmacol 2011;24(1 Suppl):23S-29S.
39. Riley T, Sontag E, Chen P, Levine A. Transcriptional control of human p53-regulated genes. Nat Rev Mol Cell Biol 2008;9:402-412. https://doi.org/10.1038/nrm2395
40. Li JJE, Muralikrishnan S, Ng CT, Yung LYL, Bay BH. Nanoparticle-induced pulmonary toxicity. Exp Biol Med 2010;235:1025-1033. https://doi.org/10.1258/ebm.2010.010021
41. Turkez H, Geyikoglu F, Tatar A, Keles MS, Kaplan İ. The effects of some boron compounds against heavy metal toxicity in human blood. Exp Toxicol Pathol 2012;64:93-101. https://doi.org/10.1016/j.etp.2010.06.011
42. Farnebo M, Bykov VJ, Wiman KG. The p53 tumor suppressor: a master regulator of diverse cellular processes and therapeutic target in cancer. Biochem Biophys Res Commun 2010;396:85-89. https://doi.org/10.1016/j.bbrc.2010.02.152
43. Rather MA, Thenmozhi AJ, Manivasagam T, Bharathi MD, Essa MM, Guillemin GJ. Neuroprotective role of Asiatic acid in aluminium chloride induced rat model of Alzheimer's disease. Front Biosci (Schol Ed) 2018;10:262-275. https://doi.org/10.2741/s514
44. Yokel RA. The toxicology of aluminum in the brain: A review. Neurotoxicology 2000;21:813-828.
45. Chen CH, Eastwood SL, Hope T, McDonald B, Francis PT, Esiri MM. Immunocytochemical study of the dorsal and median raphe nuclei in patients with Alzheimer's disease prospectively assessed for behavioural changes. Neuropathol Appl Neurobiol 2000;26:347-355. https://doi.org/10.1046/j.1365-2990.2000.00254.x
46. Litvinov D, Mahini H, Garelnabi M. Antioxidant and anti-inflammatory role of paraoxonase 1: implication in arteriosclerosis diseases. N Am J Med Sci 2012;4:523-532. https://doi.org/10.4103/1947-2714.103310
47. Brook RD, Rajagopalan S, Pope CA 3rd, Brook JR, Bhatnagar A, Diez-Roux AV, Holguin F, ET AL. Particulate matter air pollution and cardiovascular disease: an update to the scientific statement from the American Heart Association. Circulation 2010;121:2331-2378. https://doi.org/10.1161/CIR.0b013e3181dbece1
48. Seaton A, Tran L, Aitken R, Donaldson K. Nanoparticles, human health hazard and regulation. J R Soc Interface 2010;7(Suppl 1):S119-S129. https://doi.org/10.1098/rsif.2009.0252.focus
49. Chuang HC, Juan HT, Chang CN, Yan YH, Yuan TH, Wang JS, Chen HC, Hwang YH, Lee CH, Cheng TJ. Cardiopulmonary toxicity of pulmonary exposure to occupationally relevant zinc oxide nanoparticles. Nanotoxicology 2014;8:593-604. https://doi.org/10.3109/17435390.2013.809809
50. Kreyling WG, Semmler M, Erbe F, Mayer P, Takenaka S, Schulz H, Oberdorster G, Ziesenis A. Translocation of ultrafine insoluble iridium particles from lung epithelium to extrapulmonary organs is size dependent but very low. J Toxicol Environ Health A 2002;65:1513-1530. https://doi.org/10.1080/00984100290071649